

NBER WORKING PAPER SERIES

REOPENING SCENARIOS

David Baqaee
Emmanuel Farhi
Michael J. Mina
James H. Stock

Working Paper 27244
<http://www.nber.org/papers/w27244>

NATIONAL BUREAU OF ECONOMIC RESEARCH
1050 Massachusetts Avenue
Cambridge, MA 02138
May 2020

We thank Veronica De Falco, Michael Droste, Adriano Fernandes, Kathryn Holston, Stephanie Kestelman, Ed Kong, Danila Maroz, Chika Okafor, and Lingdi Xu for research assistance and James Hay for helpful discussions. The views expressed herein are those of the authors and do not necessarily reflect the views of the National Bureau of Economic Research.

NBER working papers are circulated for discussion and comment purposes. They have not been peer-reviewed or been subject to the review by the NBER Board of Directors that accompanies official NBER publications.

© 2020 by David Baqaee, Emmanuel Farhi, Michael J. Mina, and James H. Stock. All rights reserved. Short sections of text, not to exceed two paragraphs, may be quoted without explicit permission provided that full credit, including © notice, is given to the source.

Reopening Scenarios

David Baqaee, Emmanuel Farhi, Michael J. Mina, and James H. Stock

NBER Working Paper No. 27244

May 2020

JEL No. E60,I10

ABSTRACT

We use a five-age epidemiological model, combined with 66-sector economic accounting, to address a variety of questions concerning the economic reopening. We calibrate/estimate the model using contact survey data and data on weekly historical individual actions and non-pharmaceutical interventions in the weeks ending March 8 – May 16, 2020. Going forward, we model a decision-maker (governor) as following reopening guidelines like those proposed by the White House and the CDC. The sectoral accounting, combined with information on personal proximity and ability to work from home by sector, make it possible to construct a GDP-to-Risk index of which sectors provide the greatest increment in GDP per marginal increase in R_0 . Through simulations, we find that: a strong economic reopening is possible; a “smart” reopening, preferencing some sectors over others, makes only modest improvements over a broad reopening; and all this hinges on retaining strong restrictions on non-work social contacts. If non-work contacts – going to bars, shopping without social distancing and masks, large group gatherings, etc. – return only half-way to the pre-COVID-19 baseline, the current decline in deaths reverses leading to a second wave of business closures.

David Baqaee
Department of Economics
University of California at Los Angeles
Bunche Hall
Los Angeles, CA 90095
and NBER
baqaee@econ.ucla.edu

Michael J. Mina
Harvard Chan School of Public Health
Kresge Building
677 Huntington Avenue
Boston, MA 02115
USA
mmina@hsph.harvard.edu

Emmanuel Farhi
Harvard University
Department of Economics
Littauer Center
Cambridge, MA 02138
and NBER
emmanuel.farhi@gmail.com

James H. Stock
Department of Economics
Harvard University
Littauer Center M26
Cambridge, MA 02138
and NBER
James_Stock@harvard.edu

In response to the COVID-19 outbreak in March 2020, governors and local actors took sweeping measures to shut down economic and social activity in an attempt to restrain the spread of the novel coronavirus and to stem deaths. Now, as the same decision-makers begin reopening the economy, the question arises as to when and how the economy can be safely reopened

We consider two questions related to this reopening. First, focusing just on the back-to-work aspects of the reopening, how large are the gains from a staged or “smart” reopening, relative to simply reversing the shutdown and allowing (and encouraging) all businesses to reopen?

Example of nuanced reopening plans include reopening certain high-value, low-risk sectors first, and prioritizing the reentry of younger workers.

Second, what are the interactions between back-to-work policies and non-pharmaceutical interventions (NPIs) that largely focus on non-work activities? To what extent, for example, does wearing masks while shopping make room for economic expansion? Is there a quantitatively meaningful tradeoff between staging the economic reopening and relaxing guidelines regarding NPIs that primarily restrict individuals during non-work activities?

Third, reopening roadmaps (e.g., Gottlieb et al (2020), White House/CDC (2020), National Governors’ Association (2020), The Conference Board (2020), Romer (2020)) stress testing, tracing, and quarantine (or self-isolation). What is the quantitative impact of testing, tracing, and quarantine at realistic levels, given that widespread testing at the levels envisioned by the road maps remains elusive? Does testing, tracing, and quarantine provide meaningful space for the economic reopening?

To address these questions, we construct a model that combines epidemiological and economic components at a level of granularity that allows us to consider a wide range of NPIs, including ones that vary by age (such as school closings) and reopening policies that preference certain sectors. The age-based structure is important both because it allows us to consider age-based NPIs and because of the sharp mortality gradient with age for COVID-19. The epidemiological component is an age-based SEIRQD model with 5 age bins, the closest antecedent being Hay et al. (2020). The key element of this age-based model is a contact matrix that provides the

expected number of daily contacts between individuals of different ages. We use a combination of contact survey data (Mossong et al. (2017)), economic data from the BEA and BLS, Google mobility data, and miscellaneous studies such as on the efficacy of masks (Howard et al.) to construct a sequence of weekly national-average contact matrices spanning the weeks ending March 7 (the baseline) through May 16. These contact matrices are a composite of contacts at home, contacts at work, and other contacts (such as shopping and travel). The model parameters in part are drawn from the epidemiological literature and in part obtained by time series estimation of the model using observed daily death data for the US. Some parameters are weakly identified, most importantly the infection fatality rate (IFR), so in our simulations we consider a range of IFRs from 0.3% to 0.9%, with a central case of 0.6%.

The model has 66 economic sectors, in which we use measures of ability to work at home and of personal proximity while at work (Dingel and Nieman (2020), Mongey, Pilossoph and Weinberg (2020)) to differentiate worker contacts (and age) by sector. By combining the age-based epidemiological model with sectoral economics, we are able to compute a GDP-to-Risk index by sector, which measures the marginal contribution of an additional worker in a given sector to GDP, relative to the marginal contribution to the basic reproduction number R_0 .

Decision-making in this episode has been decentralized and, in general, reactive to current and recent conditions. The roadmaps and current White House guidance suggests conditioning reopening on certain observables (“gating criteria”), such as whether there is a downward trajectory in cases and deaths. Instead of adopting an optimal control approach, we therefore consider positive analysis of decision-makers (or individuals) who strive to expand economic activity while following retrospective guidelines along the lines of the roadmaps. We consider two different decision-makers – henceforth, governors – one who leans more toward prioritizing the public health measures and the other who places more weight on the economic measures.

We use this model to conduct multiple simulations. In short, we find that there is ample room for a robust recovery in economic activity – as long as it is accompanied by continued stringent personal protections outside work such as wearing masks while shopping, practicing social distancing, and limits on group gatherings. More specifically, we have three main findings:

- Smart reopening plans that focus on the nuances of returning to work can lead to modest but worthwhile improvements in economic and/or public health metrics. For example, reopening according to our GDP-to-Risk index leads to levels of output that are on the order of 0.2-1 pp higher than not using the index, for the same levels of deaths. Similarly, keeping workers who can work from home doing so, leads to a modest decrease in infections and deaths relative to bringing them back to work. Age-based work policies, such as not allowing older workers to return to the work site, holding constant their non-work contacts, have little effect on deaths but substantially retard the economic recovery.
- There is a strong interaction between non-economic NPIs and the ability of the economy to reopen. Relaxing social distancing has effects that swamp those of nuanced economic reopening plans. According to our simulations, a new normal, in which self-protective measures (social distancing, group gatherings, masks, etc.) in non-work activities are half way between the early-May shutdown and the pre-COVID-19 status quo, results in a second round of contagion and deaths, leading governors to reverse the economic reopening and prolonging the current high levels of unemployment.
- The introduction of testing, tracing, and quarantine – even if only 20% effective – provides additional room for a strong economic reopening. But such testing, tracing, and quarantine is insufficient to counteract fully the effect of relaxing of non-work personal protections.

We also consider non-economic, age-based policies. Reopening schools in the fall substantially increases the chances of a second wave of infections and deaths, putting the economic recovery at risk. There is, however, some evidence that the virus is less transmissible among children than adults, which would temper our findings, and we will learn more as other countries experiment with reopening schools under protective conditions including distancing, staggered class cohorts, etc. Of course, *not* reopening schools also presents a challenge to the economic recovery because many parents would need to stay home to provide childcare. Our simulations underscore the economic importance of finding safe ways to reopen schools in the fall. In addition, we consider

a policy of sequestering the oldest cohort (75+); we estimate that an aggressive, maintained lockdown could reduce deaths in that cohort by one-fourth, however many of the elderly's contacts are with personal service providers and extended family members at home, providing pathways for infection that can be reduced but are difficult to eliminate.

There are now many papers in the economics literature that combine epidemiological and economic models.¹ The most closely related paper to ours is Azzimonti et al. (2020). Relative to that paper, we consider the US while they focus on New York City, and we consider interactions between non-economic NPIs and economic reopening going forward rather than just an historical assessment. Some of our substantive simulations address, independently, similar questions; in particular, we have numerically close estimated values for a sector-phased reopening vs. a broad reopening, although with different models and different settings (NYC vs. US). Four other closely related papers are Çakmakli et al. (2020), who study emerging market aspects in the context of Turkey, Favero, Ichino, and Rustichini (2020), who study restarting the Italian economy, Acemoglu, Chernozhukov, Werning & Whinston (2020), who consider optimal control in a combined epidemiological/economic model with three age bins, and Rio-Chanona et al. (2020), who using sectoral input-output data to estimate the output effect of the shutdown from supply and demand shocks. We use our model to check the findings in Acemoglu et. al. (2020) concerning the value of NPIs aimed at isolating the elderly and also find they can save substantial numbers of lives, although our baseline estimates, which assume continued diligence in non-work protections, project many fewer deaths than theirs.

¹ See Acemoglu, Chernozhukov, Werning & Whinston (2020), Alvarez, Argente, and Lippi (2020), Aum, Lee, and Shin (2020), Atkeson (2020a, b), Baqaee and Farhi (2020a, b), Berger, Herkenhoff & Mongey (2020), Bodenstein, Crosetti & Guerrieri (2020), Budish (2020), Eichenbaum, Rebelo & Trabant (2020a, b), Farboodi, Jarosch, and Shimer (2020), Favero, Ichino, and Rustichini (2020), Glover, Heathcoate, Krueger & Rios-Rull (2020), Guerrieri, Lorenzoni, Straub & Werning (2020), Jones, Philippon, and Venkateswaran (2020), Krueger, Uhlig, and Xie (2020), Lin and Meissner (2020), Ludvigson, Ma, and Ng (2020), Morris et. al. (2020), Moser and Yared (2020), Mulligan (2020), Rampini (2020), Rio-Chanona, Mealy, Pichler, Lafond & Farmer (2020), and Stock (2020).

1. The Model

1.1 Age-based SEIQRD model

We use an age-based SIR model with exposed and quarantined compartments and with age-specific contact rates. An age-based approach matters for four reasons. First, death rates vary sharply by age (e.g., Ferguson et. al. (2020)). Second, workplace shutdowns affect working-age members of the population. Third, different industries have different age structures of workers, so reopening policies that differentially affect different industries could have consequences for death rates as a result of the death-age gradient. Fourth, some policies affect different ages differently, such as closing and reopening schools and only allowing workers of a certain age back into working from work.

The model simplifies Towers and Feng (2012) and follows Hay et al. (2020), adding a quarantined compartment. We consider 5 age groups: ages 0-19, 20-44, 45-64, 65-74, and 75+. The epidemiological state variables are S (susceptible), E (exposed), I (infected), Q (quarantined), and D (dead). The state variables are all 5-dimensional vectors, with each element an age group, so for example I_2 is the number of infected who are ages 20-44. The unit of time is daily. We assume that the recovered are immune or, more precisely, are immune until a vaccine and/or effective treatment becomes available.²

Let S_a (etc.) denote the a^{th} element of S (a^{th} age group). The SEIQRD model is:

$$dS_a = -\beta S_a \sum_b C_{ab} \left(\frac{I_b}{N_b} \right) \quad (1)$$

$$dE_a = -dS_a - \sigma E_a \quad (2)$$

$$dI_a = \sigma E_a - \gamma I_a - \delta_a I_a - \chi Q_a \quad (3)$$

$$dQ_a = \chi I_a - \gamma Q_a - \delta_a Q_a \quad (4)$$

² The assumption of subsequent immunity among the recovered is a matter of ongoing scientific investigation. A working hypothesis based on the related coronaviruses causing MERS and SARS is that immunity could decay but last for 1-3 years. Because our simulations run through the end of 2020, our assumption is that the recovered are immune through that period. If we are to draw conclusions beyond the simulation horizon, our assumption is that immunity lasts until a vaccine or effective treatment becomes available.

$$dR_a = \gamma I_a + \gamma Q_a \tag{5}$$

$$dD_a = \delta_a I_a + \delta_a Q_a \tag{6}$$

The total number of individuals of age a is $N_a = S_a + E_a + I_a + Q_a + R_a$.

The parameters of the model are the transmission rate β , the recovery rate γ , the latency rate σ , the age-dependent death rate δ_a , the quarantine rate χ , and the 5×5 contact matrix C , with element C_{ab} . The transmission rate β is a feature of the disease and reflects the probability of becoming infected from a close contact with an infected individual. The latency rate and death rates are also treated as functions of the disease. The death rate depends on availability of hospital services, however we do not model hospital capacity or time variation in treatment regimes and treat the death rate as varying by age but constant over time. Calibration and estimation of the model is discussed in Section 4.³

The contact matrix C is the mean number of contacts among different age groups in the population. Thus, according to equations (1) and (2), a susceptible individual of age a who comes into contact with an individual of age b has an instantaneous infection probability of β times the probability that the age- b individual is infected; the total instantaneous probability is the sum over the expected number of contacts of different ages, times the probability that the contacted individual is infected.

Underlying the stylized model of quarantine in (3) – (6) is a complex system of testing, tracing, and enforcement. Taken literally, in this model an infected individual is placed into quarantine with some probability, at which point they no longer can infect others, however they have the

³ In principle the parameters β and σ could also vary by age. There is some evidence of lower transmission among the young, however our understanding is that the scientific evidence on this is mixed and at the moment unresolved (Vogel and Couzin-Frankel (2020)). Boast, Munro, and Goldstein's (2020) evidence survey leads them to conclude that children appear to have a lower probability of becoming infected, but that there is insufficient information to conclude whether they have a different rate of transmission if they are infected, and they do not provide a quantitative estimate of the reduction in susceptibility. Also see Netherlands National Institute for Public Health at <https://www.rivm.nl/en/novel-coronavirus-covid-19/children-and-covid-19>. While the rate of detected infections among children is low, there are potential explanations other than reduced transmissibility, including less severity of the disease among the young (thus lower testing eligibility) and higher asymptomatic rates. Pending additional evidence we use the same transmission rate β for all ages however that could change as information about transmission by children becomes available.

same disease dynamics (recovery and death rates) as the non-quarantined infected. This is a stylized version of perfect quarantine with no health benefits to the quarantined individual. In practice, identifying the infected individual requires testing and tracing, and, at least in the United States, quarantine is imperfect and is more like receiving advice to self-isolate. Our simple model stands in for these complexities.

We treat the disease parameters γ , σ , and δ as time-invariant. NPIs and individual response evolve over time, and those changes induced time variation in the contact matrix C and in the quarantine rate χ . The effect of NPIs, historical and counterfactual, on C and χ are discussed in Section 3.

In a model without quarantine and with a death rate that depends on age, the initial reproductive rate R_0 is,

$$R_0 = \beta \max \text{Re} \left[\text{eval}(\tilde{C} \bullet \Gamma) \right], \quad (7)$$

where $\max \text{Re}[\text{eval}(\cdot)]$ denotes the maximum of the real part of the eigenvalues of the matrix

argument, \tilde{C} is the normalized contact matrix with elements $\tilde{C}_{ab} = (C_{ab} N_a / N_b)$,

$\Gamma_{ab} = 1 / (\gamma + \delta_b)$, and \bullet is the element-wise product (derived using the next-generation matrix method, see Towers and Feng (2012) and van den Driessche (2017)). This generalizes the familiar expression for R_0 in a scalar SIR model ($= \beta / (\gamma + \delta)$) to the case of age-based contacts with age-dependent death rates.⁴ In the special case that δ does not depend on age, (7) simplifies to,

$$R_0 = \frac{\beta}{\gamma + \delta} \max \text{Re} \left[\text{eval}(\tilde{C}) \right]. \quad (8)$$

Because δ is small relative to γ , the approximation (8) works reasonably well numerically (where

⁴ The parameters β in the scalar and age-based settings differ, where β in the scalar model is the transmission rate β in the age-based model times the expected number of contacts.

δ is the population-weighted average value of δ_a 's), and has the advantage of \tilde{C} depending on the contact matrix but no other model parameters.

1.2. Sector- and activity-based contact matrices

The contact matrix C represents the expected number of contacts in a day between individuals in different age bins. We distinguish between contacts made in three activities: at home, at work (on the work site), and other. Other includes both contacts made as a consumer engaging in economic activity, such as shopping, air travel, and dining at a restaurant, and in non-economic activities such as free recreation and social events. In a given day, an individual can be in any or all of these three states.

The expected number of contacts made in a day is the sum of the contacts made at home conditional being at home, plus those made at work conditional on being at work, plus those made while engaged in other activities conditional on doing other activities, times the respective probabilities of being in those three states. Because we are interested in differentiating between work in different sectors, which among other things differ by the degree of personal proximity and numbers of contacts at the workplace, we further distinguish between different workplace contacts. Thus, the expected number of contacts at work is the weighted average of the expected number of contacts, conditional on working in sector i , times the probability of working in sector i . We therefore have,

$$C_{ab} = p_a^{home} C_{ab}^{home} + p_a^{other} C_{ab}^{other} + \sum_{sectors\ i} p_{a,i}^{work} C_{ab,i}^{work}, \quad (9)$$

where C_{ab}^{home} is the (a, b) element of the contact matrix conditional on being at home, p_a^{home} is the probability of an age- a individual being at home, similarly for other, $C_{ab,i}^{work}$ is the (a, b) element of the contact matrix conditional on being at work in sector i , and $p_{a,i}^{work}$ is the probability of an age- a individual working in sector i .

The (unconditional) probabilities $p_{a,i}^{work}$ are the fraction of the population employed in the indicated sector:

$$p_{a,i}^{work} = \frac{L_{a,i}}{N_a}, \quad (10)$$

where $L_{a,i}$ is the number of workers of age a employed in sector i .

The disaggregation of the contact matrices in (9) allows for distinguishing the nature of contacts. A server in a restaurant will have contacts with customers in his or her capacity as a worker (work contact matrix for restaurants), while the customers will have contacts with the server in their capacity as consumers engaged in “other” activities. Similarly, a home health aide providing services to an elderly person at that person’s home will be in contact with the elderly person as part of work, while the elderly recipient will be making contacts while at home.

Estimation of the conditional contact matrices and non-work probabilities is discussed in Section 2.

1.3. Employment, unemployment, and output

Employment by age, by sector, and total (L) are respectively sums over sectors, ages, and overall:

$$L_{a,\bullet} = \sum_{sectors\ i} L_{a,i}, \quad L_{\bullet,i} = \sum_{ages\ a} L_{a,i}, \quad \text{and} \quad L = \sum_a L_{a,\bullet} = \sum_i L_{\bullet,i}, \quad (11)$$

where we use the subscript “•” to denote summation over the subscript.

The departure of output from its full-employment level is estimated using Hulten’s (1978) theorem:

$$d \ln Y = \sum_{\text{sectors } i} \Psi_i d \ln L_{\bullet,i}, \quad (12)$$

where Ψ_i is the labor income share in sector i , see Baqaee and Farhi (2020a, b) for additional discussion.

2. Data Sources

2.1. Sectoral economic data

Employment by age and industry were computed using the 2017 American Community Survey.

Dingel and Neiman (2020) and Mongey, Pilossoph, and Weinberg (2020) use O*NET data to construct an index of the fraction of workers in an occupation who can work from home (*WFH*). Mongey, Pilossoph and Weinberg (2020) construct an index of high personal proximity (*HPP*) by occupation, which measures an occupation as high personal proximity if the occupation is above the median value of proximity as measured by within-arms length interactions by occupation. These occupational measures were translated to the 66 input-output sectors using the BEA cross-walk between the 2012 NAICS and their input-output codes.

Weekly employment by industry during the period of the shutdown (the weeks ending March 14 – May 15) is estimated from hours reductions reported in the March and April Establishment surveys (Tables B1, broken down to the sectoral level proportionally to the sectoral employment changes reported in Table B2). These provide the estimates of the sectoral shocks for the Establishment Survey reference weeks (the weeks ending March 14 and April 18). For the other weeks, these sectoral breakdowns were linearly interpolated using total cumulative new claims for unemployment insurance, scaled so that the resulting labor reduction factor matches the Establishment Survey hours reduction in the reference weeks.

2.2. Contact matrices and epidemiological data

Contact matrices. The contact matrices are estimated using POLYMOD contact survey data (Mossong et. al. (2017)). Conditional contact matrices for home, other, and work were computed

by sampling contact matrices from the POLYMOD survey data and then reweighting them to match US demographics on these three activities.

We used the age distribution of workers by industry and the Mongey-Pilossoph-Weinberg (2020) personal proximity index, cross-walked to the sector level (HPP_i), to construct industry-specific conditional contact matrices, $C_{ab,i}^{work}$. We explored two methods. First, we sampled from the POLYMOD contact diary data to compute the conditional distribution (element-wise) for at-work contacts and sampled from the 15%, median, and 85% percentiles to construct low, median, and high conditional contact matrices, then assigned an industry to one of these three groups based on its HPP value. Second, we computed the mean work contact matrix, conditional on being at work, and computed industry contact matrices as the product of this mean work contact matrix and HPP , scaled by a factor such that the mean across industries (weighted by age-industry employment shares) equals the overall mean work contact matrix. These two approaches yielded similar contact matrices by sector, with most industries being low-contact and a relatively few high-contact industries. Because the total contact matrix is a mean and weighted means add but percentiles do not, it is more convenient to work with the second formulation so that is what is reported here.

The probabilities p^{other} in (9) are estimated from the POLYMOD contact data (normalized for US demographics). The probability p^{home} is nearly 1 in the POLYMOD diaries (i.e., nearly everyone spends part of their day at home) and is set to 1 for all simulations.

Epidemiological data. Daily death data, which are used to estimate selected model parameters, are taken from the Johns Hopkins COVID-19 Github repository⁵.

2.3. Calibration of Historical NPIs

We use Google mobility data and school closing data to calibrate the historical sequence of NPIs. We construct a mobility index (GMI) using two Google mobility measures at the daily level (national averages): retail and recreation, and parks⁶. These are averaged, transformed to be

⁵ https://github.com/CSSEGISandData/COVID-19/tree/master/csse_covid_19_data

⁶ <https://www.google.com/covid19/mobility/>

between 0 and 1, and standardized so that 1 represents the mean of the final two weeks of February 2020. Dates of school closings are taken from Kaiser Family Foundation (2020), aggregated to the national level using population weighting. Section 4 provides details on how these data were used to translate the NPIs into contact matrices.

3. GDP-to-Risk Index

One reopening question is whether sectors should be reopened differentially based on either their contribution to the economy or their contribution to risk of contagion. The expressions for R_0 in (8) and for output in (12) lead directly to an index of contributions of GDP per increment to R_0 . Specifically, consider a marginal addition of one more worker of age a returning to the worksite in sector i . Then the ratio of the marginal contribution to output, relative to the marginal contribution to R_0 , is,

$$\frac{d \ln Y / dL_{a,i}}{dR_0 / dL_{a,i}} \propto \frac{\Psi_i / L_i}{d \max \text{Re} [\text{eval}(\tilde{C})] / dL_{a,i}} \equiv \theta_i, \quad (13)$$

where the numerator in (13) does not depend on a because the output expression (12) does not differentiate worker productivity by age.

The derivatives in (13) depend on the current value of the contact matrix, however that dependence is numerically small (this makes sense because in the scalar case the dependence drops out, and in the matrix case it enters only by changing the eigenvectors of the normalized contact matrix, see Magnus (1985)). In addition, the expression R_0 in (7) gives the initial (base) reproduction number which might not provide a good approximation to the dynamic derivatives. We therefore also computed the ratio of derivatives in (13) by numerical differentiation of the estimated model. We found that, up to scale, the values of θ were very close to those computed using (13). For the simulations that examine sequential industry reopening, we therefore used (13), with the derivatives of $\max \text{Re} [\text{eval}(\tilde{C})]$ numerically evaluated at the baseline values of the contact matrix.

A useful feature of θ is that, up to scale, it does not depend on epidemiological parameters other than the contact matrix. Without these parameters the units of θ are not meaningful so for convenience we standardize θ to have mean zero and variance 1 across sectors (equal-weighted).⁷ We call this standardized version of θ the GDP-to-Risk Index.

The values of the GDP-to-Risk index θ are listed in Appendix Table 1 for the 66 NAICS-code private sectors in our model. Generally speaking, the highest GDP-to-Risk sectors are white collar industries such as insurance and computer design, along with some high-value moderate-risk production sectors such as oil and gas extraction and primary metals production. Moderate GDP-to-Risk industries include paper products; forestry and fishing; and utilities. Low GDP-to-Risk industries are generally ones with many low-paid employees who are exposed to high levels of personal contacts at work, including nursing and residential care facilities; food services and drinking places; social assistants; gambling and recreational industries; transit and ground passenger transportation; and educational services.

4. Calibration of Historical NPIs and Estimation

The NPIs that were implemented between the second week of March and mid-May include: closing schools; exhibiting personal distancing; prohibiting operation of many businesses and making changes in the workplace to reduce transmission in others; in some localities, issuing stay-at-home orders; orders against large gatherings, where the threshold varied across jurisdiction and over time; wearing masks and gloves; and urging self-isolation among those believed to have come in close contact with an infected individual.

⁷ Three sectors are outliers in their value of θ , having large contributions to GDP relative to risk: Securities, commodity contracts, and investments; Legal services; and Management of companies and enterprises. To avoid a conclusion that the optimal reopening strategy was to put the lawyers and managers back to work, but not production workers, we truncated the values for these sectors to be the same as the fourth-highest value of non-truncated θ , and computed the standardized index after this truncation.

These NPIs, along with personal behavioral adaptations in response to the virus, enter the model through the contact matrix. We introduce these NPIs through the following contact matrix parameterization:

$$C_{ab} = \lambda_{home} P_a^{home} C_{ab}^{home} + \lambda_{SD} \lambda_{other,a} P_a^{other} C_{ab}^{other} + \lambda_{work} \sum_{sectors\ i} s_i (1 - \lambda_{wfh} WFH_i) P_{a,i}^{work} C_{ab,i}^{work}. \quad (14)$$

The λ factors are all between 0 and 1 and model contact reductions through behavioral or mandated changes: λ_{home} models reduced contacts at home; λ_{SD} models reduced close contacts in other activities (shopping, social) through social distancing and wearing masks and/or gloves; $\lambda_{other,a}$ models age-based reduced contacts in other activities (for example, not going out to bars or restaurants); λ_{work} models changes in the work place that reduce in-work contacts; λ_{wfh} represents the share of those able to work from home who actually do so; and WFH_i is the Dingel-Nieman index (cross-walked to NAICS sectors) of the fraction of workers in sector i who are able to work from home. These factors enter multiplicatively. For example, λ_{home} is the fractional number of contacts at home, compared to the February 2020 baseline. All these factors in general vary over time, so the resulting contact matrix varies over time.

The factor s_i is the fraction of employees in sector i who are still employed and working, specifically, at time t ,

$$s_{it} = L_{\bullet,i,t} / L_{\bullet,i,t_0}, \quad (15)$$

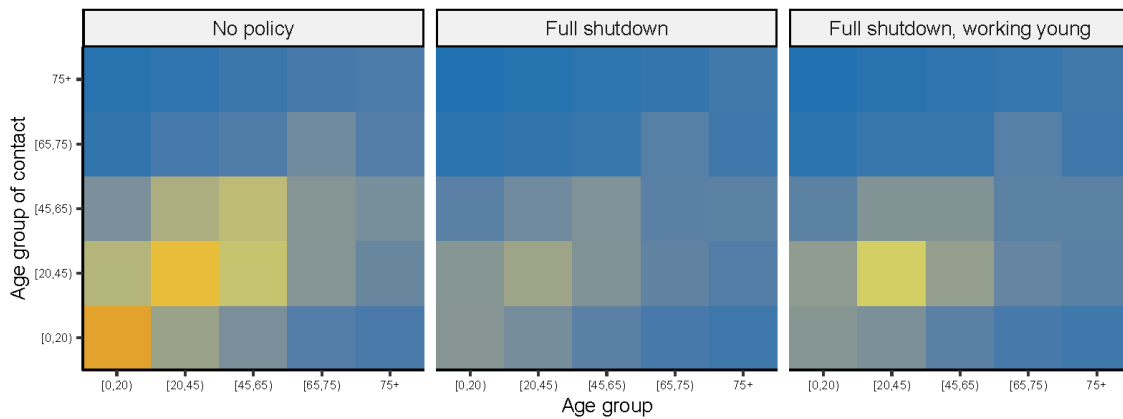
where $L_{\bullet,i,t}$ is the all-ages labor force in industry i at date t and t_0 is the final week in February 2020.

We make two uses of these factors. The first is to construct a sequence of weekly historical contact matrices from the end of February through the second week of May, 2020, with the end of February and the first week of March being the baseline and the remaining contact matrices reflecting NPIs and behavioral responses. The second is to consider manipulations of the factors

in counterfactual simulations. We discuss the construction of historical contact matrices in Section 4.1 and the counterfactual applications in Sections 5 and 6.

Figure 1 illustrates three different contact matrices under the no-policy baseline, a full shutdown scenario, and a hypothetical shutdown that allows workers aged 20-45 to return to work. Under everyday circumstances, contacts vary substantially by age, with the greatest contacts among the young and among those ages 20-45. These contacts are reduced as the economy shuts down or partially reopens.

**Figure 1. Illustrative contact matrices:
Baseline, full shutdown, and counterfactual age-based work**



4.1. Historical contact matrices

The historical exercise entails using available data to calibrate the λ and s factors in (14) to construct a sequence of weekly contact matrices over the shutdown. Because of the novelty of COVID-19 and despite active research by epidemiologists, medical researchers, and economists, little is known about many of these parameters. We therefore calibrate them using what information is available, cognizant of the heterogeneity of local decisions and behavior across the US during this period.

Reductions in work contacts arise from workers being laid off or on furlough, and if they are able, from working at home. The estimation of the weekly sequence of total reduction in hours by sector is discussed in Section 2.1 and this sequence was used for s_i . Of those remaining at work, a fraction λ_{wfh} of those able to work from home were assumed to be, in fact, working from

home. Data on this fraction are currently unavailable and absent such data, we assume that this fraction jumped to 75% in the week ending April 4 and reached 90% by the week ending May 9.

For the effect of other-activity social distancing historically, we use the Google mobility index (described in Section 3) as a direct estimate of $\lambda_{other,a}$ for $a \geq 2$ (that is, historically $\lambda_{other,a} = GMI$ for the week in question, $a \geq 2$).

School closings result in reducing the contact children have with others, that is, in reducing $\lambda_{other,1}$. We set $\lambda_{other,1}$ to equal the population-weighted actual average of open schools by week for the US, with a floor reflecting non-school interactions.

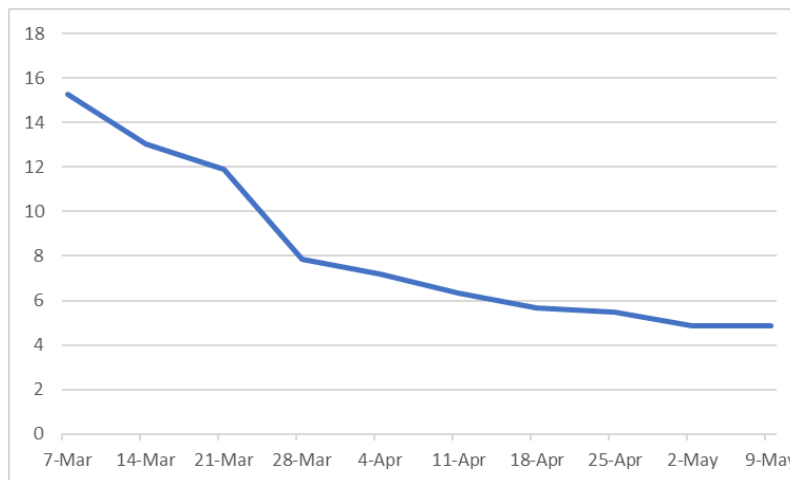
The factor λ_{SD} encompasses the use of social distancing and other personal NPIs, in particular masks and gloves, during non-work, non-home activities. We are not aware of time series data on the prevalence of mask usage during the epidemic. Until April 3, the CDC recommended that healthy people wear masks only when taking care of someone ill with COVID-19. On April 3, the CDC changed that guidance to recommend the use of cloth face coverings. Masks do not appear to have been in widespread use, even in the hardest-hit states, until more recently. For example, New York implemented a mandatory mask order on April 15, Bay Area counties did so on April 22, Illinois on May 1, Massachusetts on May 6, and many states have not required masks although some businesses working in those states have. The effect of masks on COVID-19 transmission has been reviewed by Howard et. al. (2020) and they suggest $\lambda_{mg} = (1 - ep_m)^2$, where e is the efficacy of trapping viral particles inside the mask and p_m is the percentage of the population wearing the mask. They suggest considering 50% usage and 50% efficacy, which yields $\lambda_{mg} = 0.5625$. We model masks as phasing in starting the week ending April 11. Other social distancing started phasing in earlier. Combining the effects of masks and gloves with these other social distancing measures leads us to set λ_{SD} as falling to 0.45 by the week ending May 9.

Concerning NPIs at the work site, here too we are not aware of survey data documenting practices or prevalence, however public guidance and requirements provide a guide to the extent and timing. For establishments that remained open, state and/or business actions to implement personal distancing included restricting restaurants to takeout or delivery, capacity limits at

restaurants, masks and shields at work, adding manufacturing shifts to de-densify the work site, requiring changes in practices at construction sites to reduce close contacts, and otherwise de-densifying work sites. In addition to state orders, some employers took such steps voluntarily. It appears that many of these actions happened shortly after the President declared a state of emergency on March 13, and those actions continued. We model those combined actions as having the effect, by the week ending May 9, of reducing workplace contacts by half, among those workers who are still working at the work site.

Figure 2 shows the largest real part of the eigenvalues of the normalized contact matrix for the weeks ending March 7 (the no-NPI benchmark week) through the week ending May 9, the final week for which we have unemployment insurance data and Google mobility data. The largest eigenvalue fell sharply in late March, associated with the closing of schools in the week ending March 21 and the massive job losses in that and the next week. Despite the rising measures of unemployment in the economy, it declined only marginally since late April into May as people increased other activity as measured by the Google mobility index discussed in Section 2.

Figure 2. Maximum real part of the eigenvalues of the normalized contact matrix \tilde{C} , weeks ending March 7 – May 9.



Notes: Author’s construction based on calibration of contact matrices using NPIs as discussed in the text.

4.2. Epidemiological parameters and Estimation

We adopt the values from Kissler et al. (2020) for γ and σ , specifically a latency period of 4.6 days and an infectious period of 5 days. We parameterize the mortality rate δ as proportional to the values in Ferguson et al. (2020), where the constant of proportionality is determined by the infection-fatality rate (IFR). The parameter β is determined by from R_0 from (7), using the baseline (February 2020) contact matrix and an assumed value of the IFR. Given assumed values of R_0 and the IFR, the remaining free parameter is the initial number of infections at the first date of our model evaluation (February 21, 2020).

The no-NPI period for the infection is brief, with our calibrated sequence of NPIs starting to have effect in mid-March as seen in Figure 2. As a check on the NPI construction, we introduce a free parameter φ multiplying the contact matrices starting the week ending March 14. Thus, given values of R_0 and the IFR, the model has two free parameters, the initial number of infections I_0 and φ . The daily deaths data are noisy and exhibit strong weekly patterns which would not be fit by the model. We therefore estimate the parameters by least squares fit to rolling 7-day cumulative deaths data for 7-day periods ending March 8 – May 15.

Table 1 summarizes estimated values of φ and I_0 for various values of R_0 and the IFR. We are not aware of applicable distribution theory, which is likely to be complicated because of the strongly serially correlated data, so we do not report standard errors. The final column reports the RMSE (units are thousands of deaths).

Figure 3 plots actual weekly deaths and predicted weekly deaths from the estimated model for values of R_0 over the grid 2.45, 2.55, ..., 3.05 and for the IFR over the grid 0.3%, ..., 1.0%.

We note five features of the results. First, the model largely tracks the weekly deaths data. Although the model overpredicts deaths in March, there is evidence that deaths due to COVID-19 have been under-reported, especially early in the epidemic⁸; the model fit is consistent with that early underreporting.

⁸ See for example the excess deaths Web sites by the Centers for Disease Control at https://www.cdc.gov/nchs/nvss/vsrr/covid19/excess_deaths.htm and by the New York Times at <https://www.nytimes.com/interactive/2020/04/21/world/coronavirus-missing-deaths.html>.

Second, the model fit is nearly identical for a large range of values of R_0 and the IFR. Substantively, values of R_0 of 2.45 and 3.05 have extremely different dynamics over the full (uncontrolled) course of an epidemic, and the IFRs consider vary by more than a factor of 3. But the predicted values are evidently virtually identical. In econometrics terminology, the parameters R_0 (or, equivalently, β) and the IFR (or, equivalently, the scale parameter on δ) are weakly identified as pointed out by Atkeson (2020b).

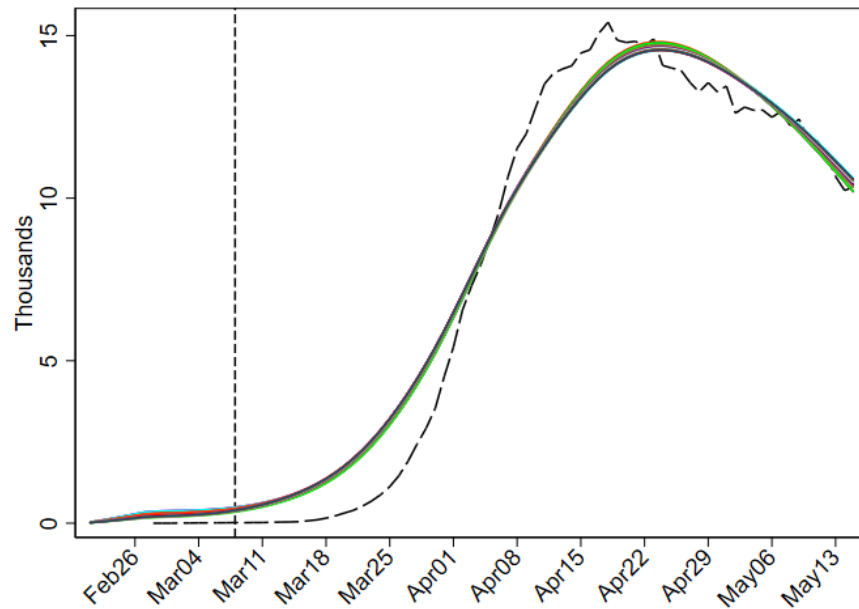
Third, the estimated values of φ are generally around 1, providing a validation of the calibration used to construct the historical NPIs.

Table 1. Estimated values of initial infections and φ , given R_0 and the IFR

R_0	IFR	\hat{I}_0	$\hat{\varphi}$	RMSE
2.45	0.003	10013	1.055	1.0468
2.45	0.006	5557	1.026	1.1099
2.45	0.009	3826	1.019	1.1302
2.65	0.003	7998	0.976	1.0437
2.65	0.006	4527	0.947	1.1075
2.65	0.009	3047	0.943	1.1270
2.85	0.003	6456	0.907	1.0414
2.85	0.006	3599	0.882	1.1042
2.85	0.009	2443	0.878	1.1248
3.05	0.003	5243	0.848	1.0395
3.05	0.006	2923	0.825	1.1020
3.05	0.009	2016	0.818	1.1222

Notes: The parameters I_0 and φ are respectively the initial number of infections on Feb. 21 and a scaling factor multiplying the calibrated sequence of contact matrices from March 14 through May 15. Given the listed values of R_0 and the IFR, the parameters are estimated using data on 7-day cumulative deaths (units: thousands) from March 8 through May 15.

Figure 3. Weekly deaths, actual and predicted, for $2.45 \leq R_0 \leq 3.05$ and $0.3\% \leq \text{IFR} \leq 1.0\%$



Notes: Estimation period March 8, 2020 – May 15, 2020

5. Reopening Plans

We model reopening plans as reacting to recent developments with the twin aims of controlling deaths and reopening the economy in mind. In so doing, we treat governors as following the CDC and White House reopening guidelines (White House, April 16, 2020), which advises reopening the economy if there is a downward trajectory of symptoms and cases for 14 days, along with having adequate medical capacity and healthcare worker testing. Because confirmed cases are a poor measure of total infections (because of rationed testing and changes in test availability), we instead focus on 14 days of declining deaths as the indicator to follow in the White House/CDC reopening guidelines.

Specifically, we consider a governor who will: restrict activity when deaths are rising or high, relax those restrictions when deaths are falling or low, tend to reopen when the unemployment rate is high, and tend to reopen when the cumulative unemployment gap is high. This final

tendency reflects increasing pressures on budgets – personal, business, and public – from an additional month of high unemployment and low incomes on top of previous months.

In the jargon of control theory, the governor follows a proportional-integral-derivative (PID) control rule, in which the feedback depends on current deaths, the 14-day change in deaths (declining death rate), the current unemployment rate, and the integral of the unemployment rate. Accordingly, we suppose that the governor follows the linear PID controller,

$$u_t = \kappa_0 + \kappa_{up} U_{t-1} + \kappa_{ui} \int_{t_0}^{t-1} U_s ds + \kappa_{dp} D_{t-1} + \kappa_{dd} \dot{D}_{t-1}, \quad (16)$$

where U_t is the unemployment rate ($= 1 - L_t / L_{t_0}$, where t_0 is the end of February 2020) and \dot{D} is the time derivative of the death rate. The CDC recommends tracking not the instantaneous derivative of infections (or D) but the change over 14 days, and deaths are noisy suggesting some smoothing of D . Similarly, U is unobserved and at best can be estimated with a lag, even using new and continuing claims for unemployment insurance and nonstandard real-time data. For the various terms on the right-hand side of (16) we therefore use, in order: the 14-day average of the unemployment rate, the cumulative daily unemployment rate since March 7, deaths over the previous two days (these are observed without noise in our model), and the 14-day change in the two-day death rate.

The decision facing the decision maker is whether to allow individuals back to work and to shopping, as well as to relax non-work NPIs. We treat the final week of February 2020 as full employment so at most any reopening can achieve that level of employment, that is, reopening is bounded; accordingly, we use a sigmoid to bound the linear controller in (16) between zero and one.

In addition, reopening can be staggered across industries, in particular we consider the possibility of reopening industries differentially by sector based on their GDP-to-Risk index. A narrow interpretation of the GDP-to-Risk index would reopen industries sequentially in order of the value of the index. This is unrealistic so instead we consider a phased reopening in which all

industries reopen, some faster than others. We therefore consider a sequence of sectoral reopenings as determined by the PID controller, shifted by the GDP-to-Risk index:

$$s_{it} = s_{it_R} + \Phi(u_t + \kappa_\theta \theta_i)(1 - s_{it_R}), \quad (17)$$

where s_{it} is the workforce in sector i at date t as a fraction of its original workforce, see (15), t_R is the initial date of the reopening, and Φ is the cumulative Gaussian distribution. (The cumulative Gaussian plays no intrinsic role other than as a sigmoid to restrain the controller to be between 0 and 1.) The industry shifter $\kappa_\theta \theta_i$ preferences industry i based on its GDP-to-Risk index.

Finally, reopening the economy requires not just workers but shoppers. In the shutdown phase, the factor $\lambda_{other,a}$ for $a > 2$ was set to equal the Google mobility index. We model this factor as increasing to 1 based on the increase in GDP arising from the additional production as the economy reopens, so that full employment corresponds to $\lambda_{other,a} = 1$ for $a > 2$.

Non-economic NPIs. The other NPIs – reopening school, social distancing, wearing masks, etc. – are either under the control of the governor (reopening schools) or are decisions made by individuals that are influenced by the governor. Instead of specifying policy paths for these other NPIs, we examine different scenarios in which the governor behaves according to (16) and (17) concerning sectoral reopening. For example, one set of scenarios entails opening up schools, but with protections; another entails relaxing social distancing by increasing λ_{SD} (reflecting either policy or noncompliance), and a third examines allowing λ_{wfh} to evolve reflecting workers returning to the workplace.

6. Simulation Results

Our simulations consider two baselines: a slow economic reopening plan, reflecting a governor driven more by health than economic considerations, and a faster economic reopening, in which relatively more weight is placed on economic considerations. We then consider two sets of variations off these baselines: the first considers policies (or actions) affecting economic

reopening and going back to work, holding constant non-economic NPIs, and the second considers non-economic NPIs such as reopening school and relaxing social distancing.

Our simulations have the lifting of the shutdown beginning on May 18. This represents a compromise, with some localities starting the reopening earlier (Georgia for example allowed reopening of most consumer-facing businesses on April 24) and others reopening later (for example, Massachusetts, Michigan, and New York City). The reopenings are also partial, for example as of May 16, all but one state (Montana) has full-year school closures required or recommended. The business reopenings also vary widely, with some states allowing non-essential businesses to reopen but at reduced capacity.

All simulations reported here are for $R_0 = 2.45$, with results shown for $0.3\% \leq \text{IFR} \leq 0.9\%$. The simulation results are relatively insensitive to R_0 because under all scenarios the driver of the effective reproduction number, the maximum real eigenvalue of the normalized contact matrix, is controlled by the policy-maker/individual behavior according to (16) and (17).

All simulations end on January 1, 2021.

6.1. Baseline scenarios

Baseline results for the slow and fast reopening scenarios are given in Figure 4 and Figure 5, respectively. In both scenarios, businesses are allowed to reopen according to a schedule implemented by the governor according to the PID control rule. In addition, shoppers return to stores in proportion to the increase in GDP. However, all other economic and non-economic are held constant at their baseline values as of just before the reopening (i.e., the final values of the calibrated historical NPIs). In particular, the use of social distancing, masks and gloves, and restraint in home contacts is unchanged from their shutdown values, and schools do not reopen. In addition, the governor does not prioritize one industry over another in the reopening.

The left panel of each figure depicts the path of weekly deaths and the monthly unemployment rate, where the unemployment rate is calibrated to lost hours as a percent of the February 2020 work force with a full-employment unemployment rate of 3.5%. The right panel shows weekly

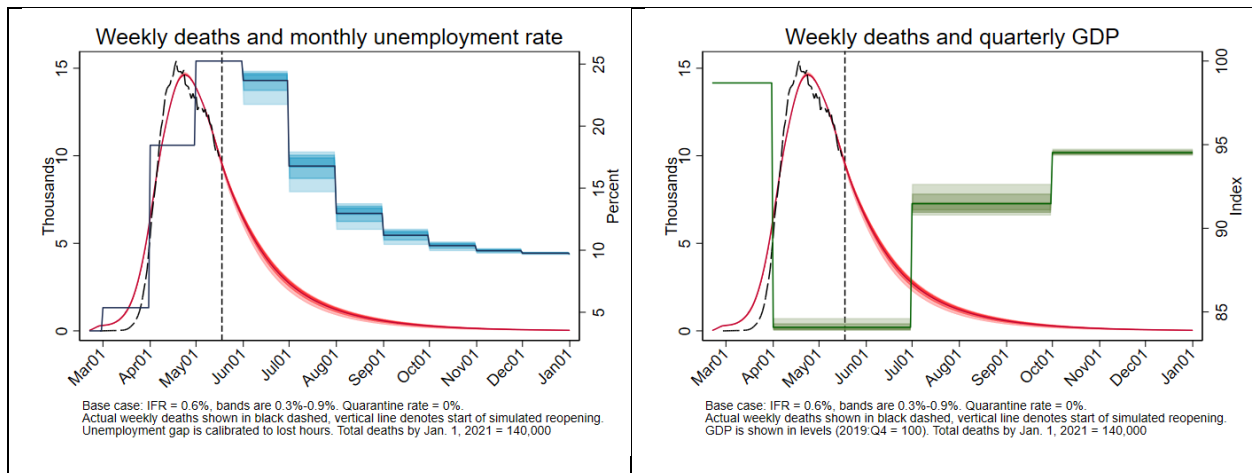
deaths and the level of quarterly GDP, indexed to equal 100 in the fourth quarter of 2019. The central case in the fans is for IFR = 0.6%, with the shaded regions representing IFR = 0.3%, to 0.9% in 0.1 percentage point increments. The total number of deaths through January 1, 2021 is given in the figure notes for IFR = 0.6%.

Under both baselines, the number of weekly deaths tends to zero by the end of the fall, with total deaths by Jan.1 of 140,000 under the slow reopening and 157,000 under the fast reopening for the IFR=0.6% case. These estimates are within the range (but on the low side) of estimates from other models, for example the IHME model currently is projecting 147,000 deaths by August 1⁹. The economic indicators vary substantially between the two reopening plans, however, with economic slack all but disappearing by the end of the summer under the fast reopening plan, but the unemployment rate remaining just below 10% under the slow reopening plan.

Figure 6 provides shows age-based information on total deaths and the share of recovered individuals by age. Of the 140,00 deaths by Jan. 1, 50,000 are among those ages 75+. By Jan. 1, only 8% of the population has been infected, with those ages 20-54 having the highest recovered rates because of low death rates combined with higher rates of contact.

The remaining simulations vary the assumptions of this reopening baseline.

Figure 4. Slow reopening baseline



⁹ <https://covid19.healthdata.org/United-States-of-America>, accessed May 17, 2020.

Figure 5. Fast reopening baseline

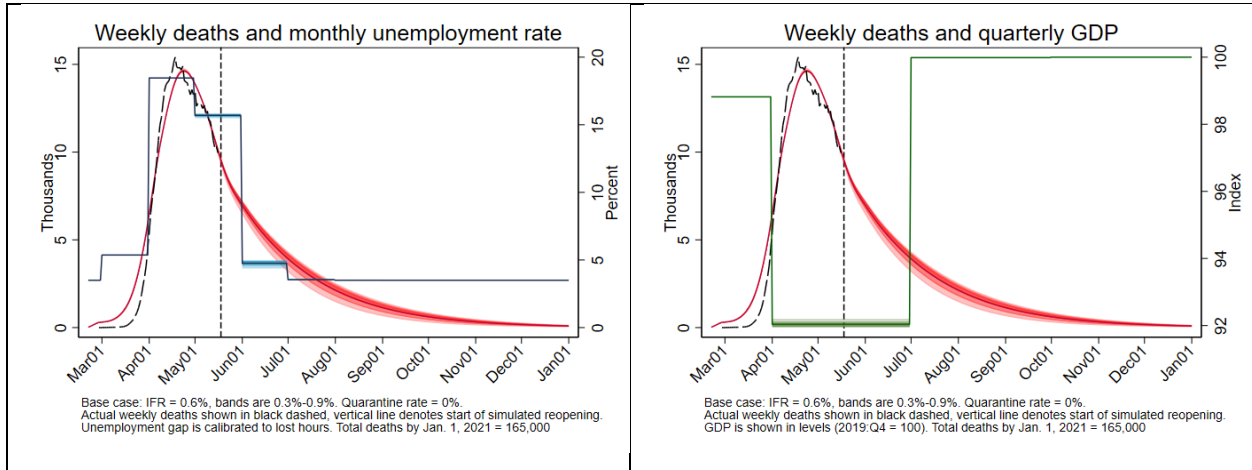
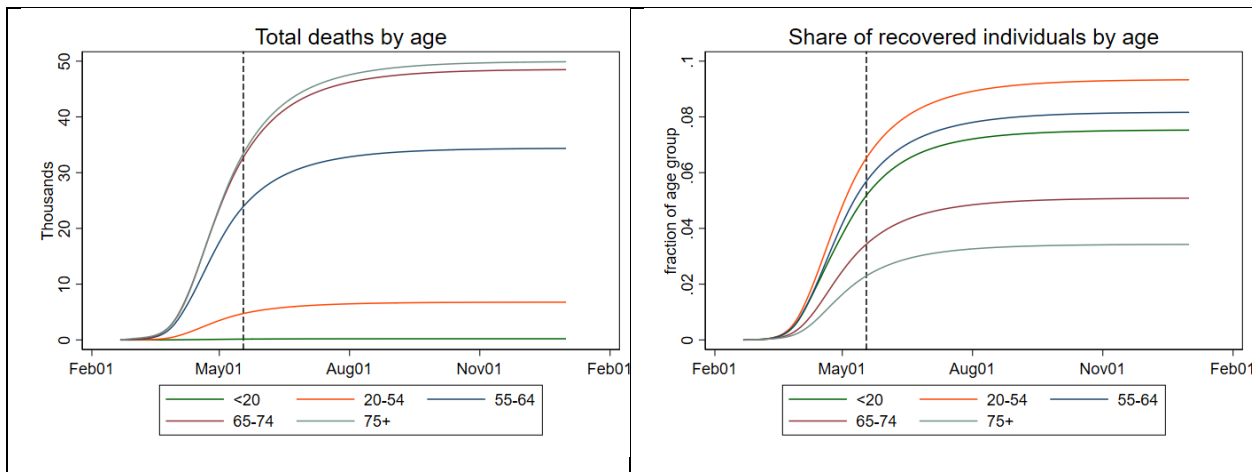


Figure 6. Deaths and share of recovered by age, slow reopening baseline



6.2. Alternative economic reopening scenarios

The baseline reopening scenarios do not prioritize sectors for reopening. The effect of instead prioritizing sectors based on their GDP-to-Risk index is shown in Figure 7.¹⁰ In this scenario, deaths are held constant, the unemployment rate rises by approximately 0.1 pp (slightly fewer workers return to work than in the non-prioritized case, but they are more productive), and GDP

¹⁰ We conducted a series of experiments in which κ_θ in (17) was varied on a grid, holding constant the unemployment rate. The results of this experiment are not monotonic in κ_θ because of the full-employment bound: in our (17), a very large value of κ_θ would open only the highest value-to-risk industries. We found that setting $\kappa_\theta = 0.75$ resulted in the greatest increase in GDP holding constant deaths, under the slow reopening control rule parameters.

is higher by 0.2 pp, 0.9, and 0.7 percentage points higher in the second, third, and fourth quarters of 2020, respectively.

Compared to the collapse of output during the shutdown, the gains from prioritizing industries based on the GDP-to-Risk index are small, however those gains are positive and moreover they reflect discussions of reopening schedules in some of the roadmaps. We therefore adopt industry preferencing (with $\kappa_\theta = 0.75$) for the remainder of the simulations.

Figure 8 considers an age-based reopening policy, in which only workers under age 65 are allowed back to work; those 65 and older work from home if they can. The effect of this NPI on employment and contagion varies by sector, depending on the age distribution of workers, personal proximity in the workplace, and the extent to which that sector admits working from home. In both the fast and slow reopening scenarios, this NPI produces a substantially greater unemployment rate (5.4 pp higher) and substantially lower GDP. In the slow reopening scenario the reduction in deaths is small (2000 fewer deaths by Jan. 1), but is greater in the fast reopening scenario (17,000 fewer). The reason for the relatively small reduction in the death rate is that the only restrictions this NPI places on older workers is that they must work from home, or not at all, in particular it does not restrict their non-work activities. Because workplace contacts are only a fraction of the total contacts that these older workers have, the older workers become infected at nearly the same rate, just through non-work contacts. This small reduction in contacts comes at a substantial economic cost because they are excluded from the on-site labor force.

The scenarios so far do not have workers returning to the workplace if they are able to work from home. Figure 9 and Figure 10 consider workers gradually returning to the work site under the slow and fast scenarios, respectively, so that by Jan. 1 only 10% of those able to work from home are doing so. Under the slow control rule, there is an increase of 5,000 deaths, which retards the reopening, leaving the unemployment rate higher by 1.0 pp by Jan. 1. Under the fast rule, deaths rise by 7,000, however this does not substantially retard the more aggressive reopening policy. We note that there are plausibly effects on productivity from working at home, although *a-priori* the overall sign is unclear. Workers save time in commuting, however they could have distractions such as from child care. Bloom et al. (2015) find that workers who work

from home are more productive, however that is a pre-COVID19 study so there is plausibly selection in those results (see Mas and Pallais (2019) for a review). The main implication here is that the effects on deaths of workers returning to the workplace – even one with protections – are relatively small but could be sufficient, under a cautious governor, to retard the reopening.

Figure 7. Reopening based on GDP-to-Risk index, slow reopening baseline

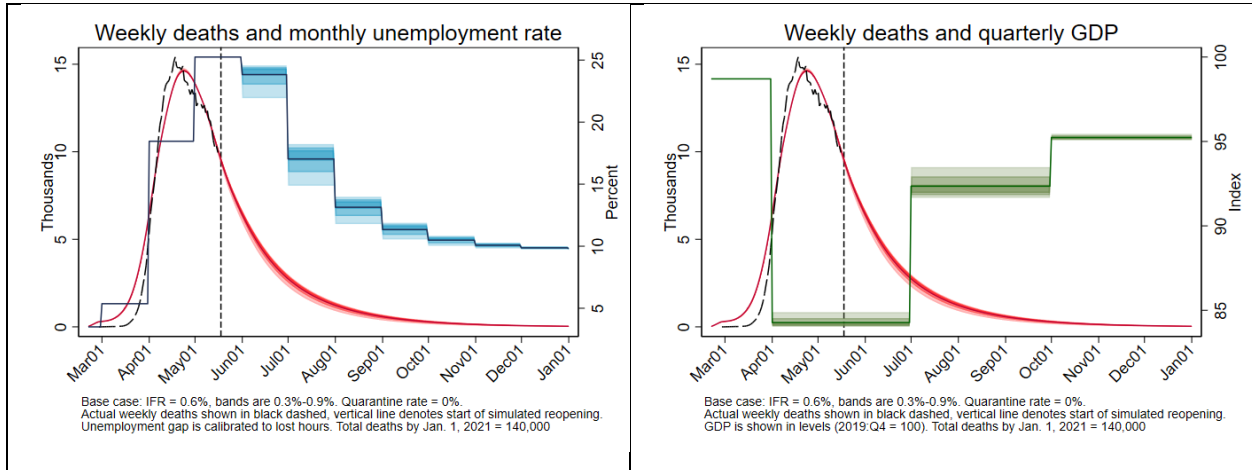


Figure 8. Workers aged <65 only, slow (left) and fast (right) baselines

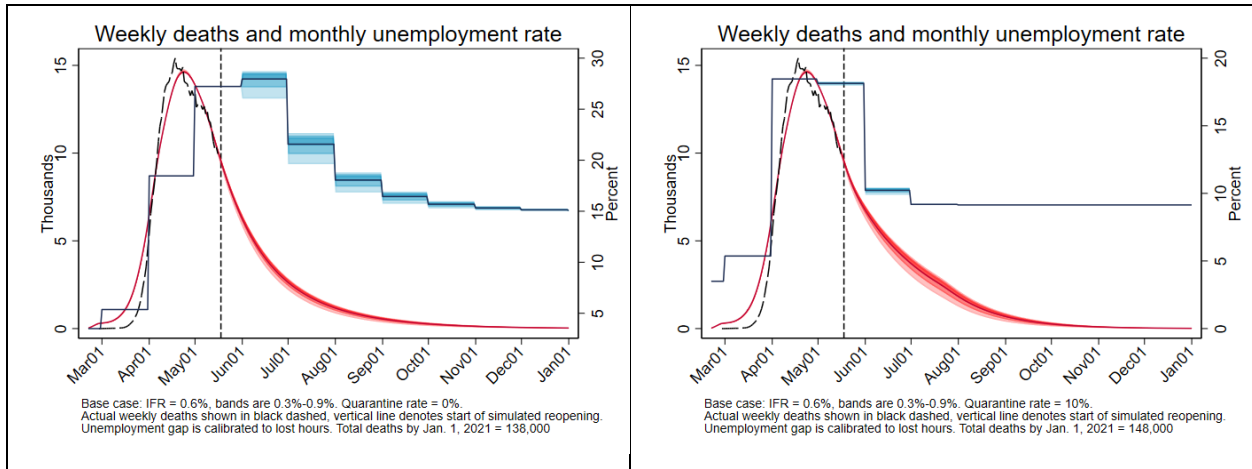


Figure 9. Gradually returning to the workplace, slow reopening baseline

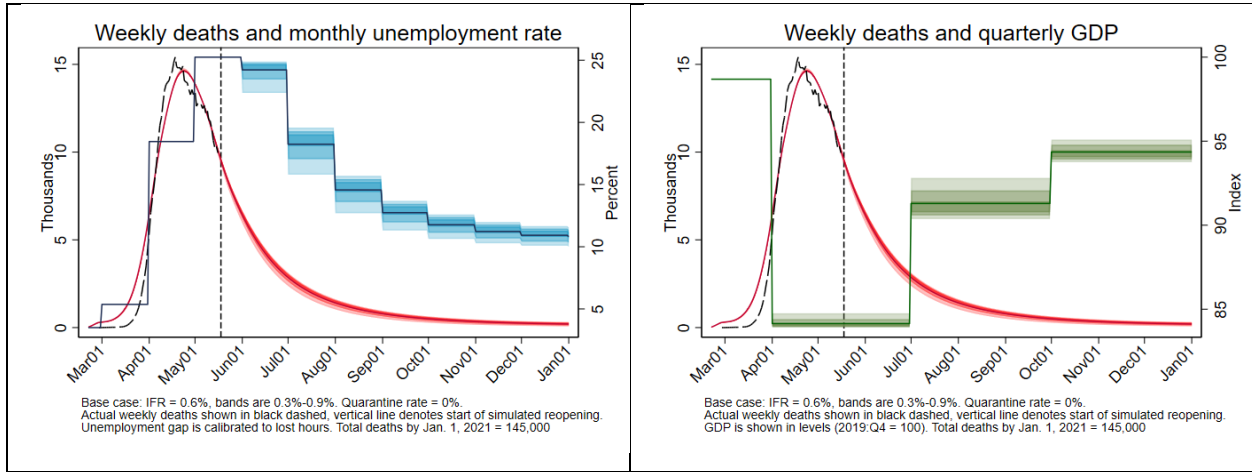
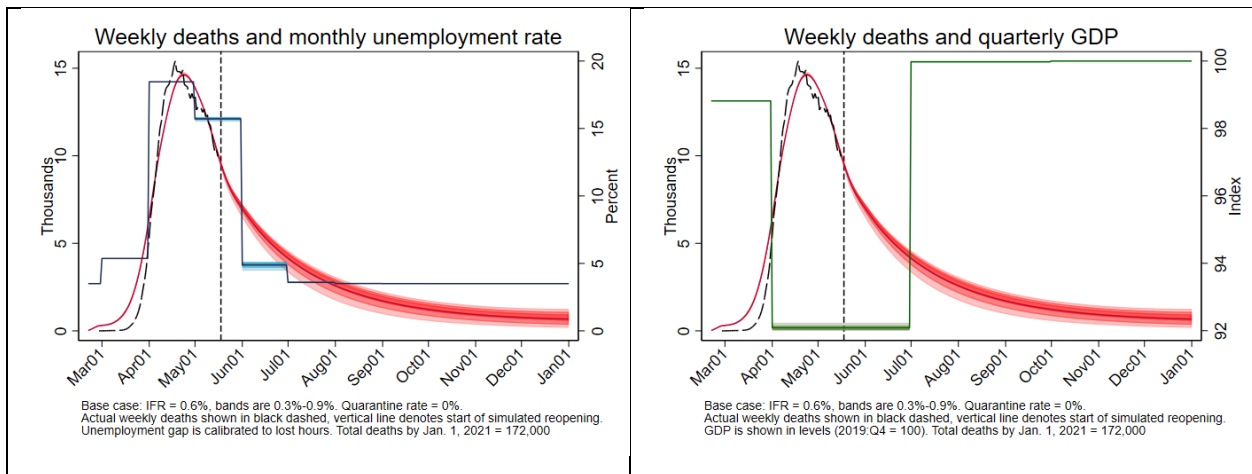


Figure 10. Gradually returning to the workplace, fast reopening baseline



6.3. Non-economic NPIs

We now examine the interaction between non-economic NPIs and economic ones in the reopening. We begin by considering relaxing the stringent personal protection policies in place in non-work activities (home and other) in mid-May. For non-work, non-home activities, we consider a reduction in the stringency of social distancing equivalent to a two-thirds reduction in the use of masks (using the mask effectiveness formula in Section 4); this amounts to an increase in λ_{SD} from 0.4 to 0.75. This increase need not be solely due to a reduction in masks but rather accounts for all other measures of non-work, non-home self-protection, including attending non-work group activities, not respecting social distancing while shopping, and so forth. (Recall that

the baseline economic expansion already introduces more shopping, here the variation is on personal protections while engaged in shopping and other activities.) For home, the restrictions in home contacts (parties etc.) are reduced half-way to the pre-COVID-19 normal. Thus, these reductions in non-work activities represent a partial adjustment to a social new normal, returning roughly half-way to the pre-crisis level of contacts from the most restrictive point in the shutdown.

The results of relaxing these personal protections are shown in in Figure 11. Under both the fast and slow governors, there is a strong upsurge in deaths a few weeks after the reopening. The slow governor responds aggressively by shutting down the economy again. The fast governor responds by scaling back the economic reopening. By August 1, in the slow scenario there are 220,000 deaths, at the high end of the current IHME projections, and 421,00 deaths by January 1. In the fast scenario, there are 726,000 deaths by Jan. 1.

Figure 12 considers reopening schools in the fall, with protections in place in schools so that the number of contacts made in school is reduced by half, relative to the pre-COVID-19 baseline. Here, adult non-work self-protective measures are kept at the same levels as in mid-May. In both the fast and the slow scenarios, there is an increase in infections and deaths in the fall, although it is greater in the fast case. In both the fast and slow cases, the increase in deaths induce the governors to tighten up and close some businesses (the lowest GDP-to-Risk sectors first), leading to a W-shaped recession.

Figure 13 considers reopening schools, with the same at-school protections as in Figure 12, except that adult non-work self-protective measures relax to roughly one-half their pre-COVID-19 levels. Thus Figure 13 represents a “new normal” in which students return to school, but with restrictions, and social distancing is practiced by shoppers, at parks, and so forth. In this new normal, the restrictions are half-way between those of mid-May and those pre-COVID-19. In the slow scenario, the weekly death curve is flattened but does not decline. The slow governor never reopens and the recession extends through the end of the year. In the fast scenario, after a dip, the weekly death rate doubles, and even the fast governor delays reopening businesses until the fall after a short period of reopening in late May and early June.

We stress that the uncertainty surrounding the school reopening scenarios is especially high because of the lack of knowledge about transmissibility of the virus by the young. As discussed in footnote 3, there is some evidence that children transmit the virus less than do adults; if so, the resurgence of the virus with school reopenings in Figure 12 and Figure 13 would overstate the contribution to risk of reopening schools.

Figure 11. Relaxing non-work social distancing, slow (left) and fast (right) baselines

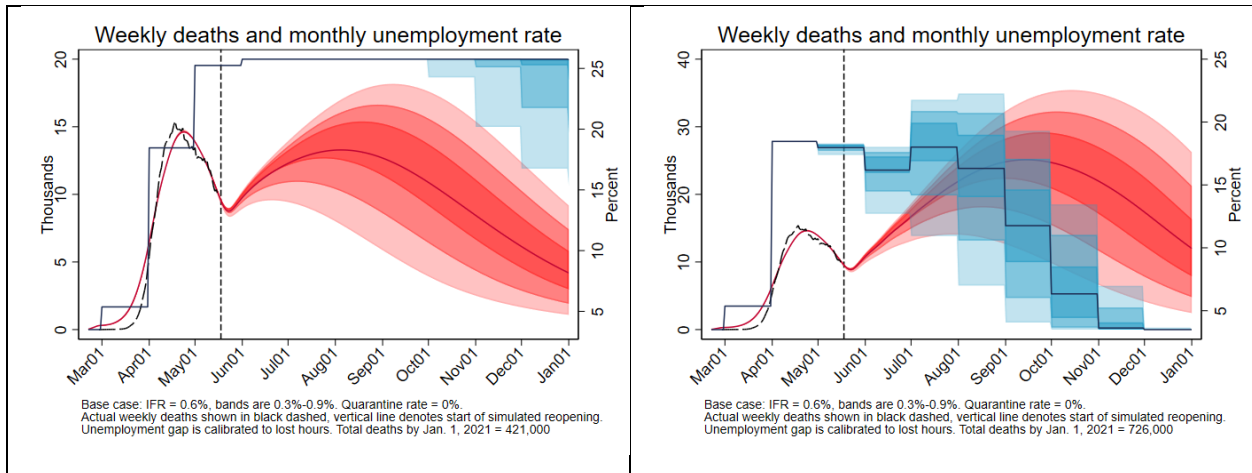


Figure 12. Reopening schools with protections, slow (left) and fast (right) baselines

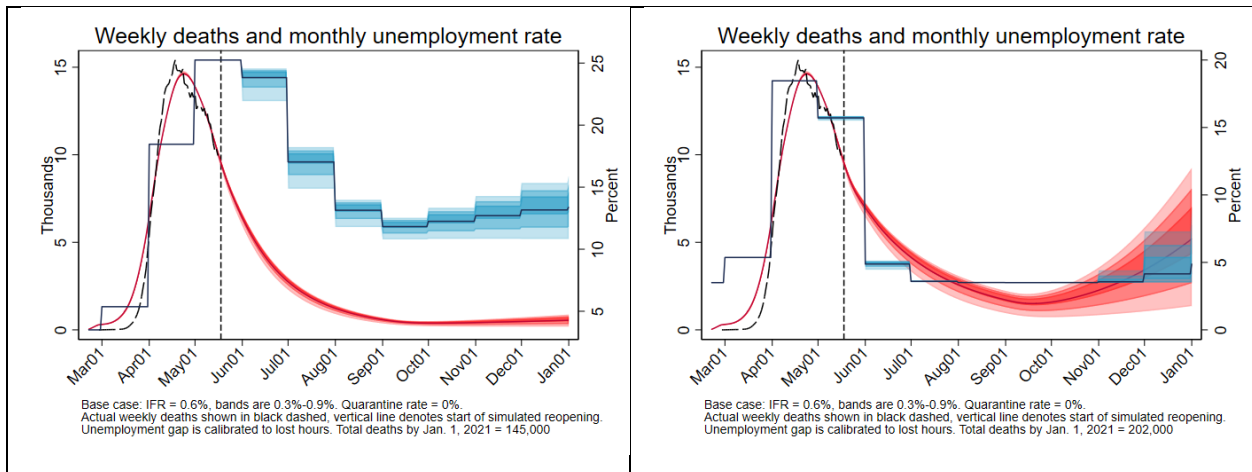
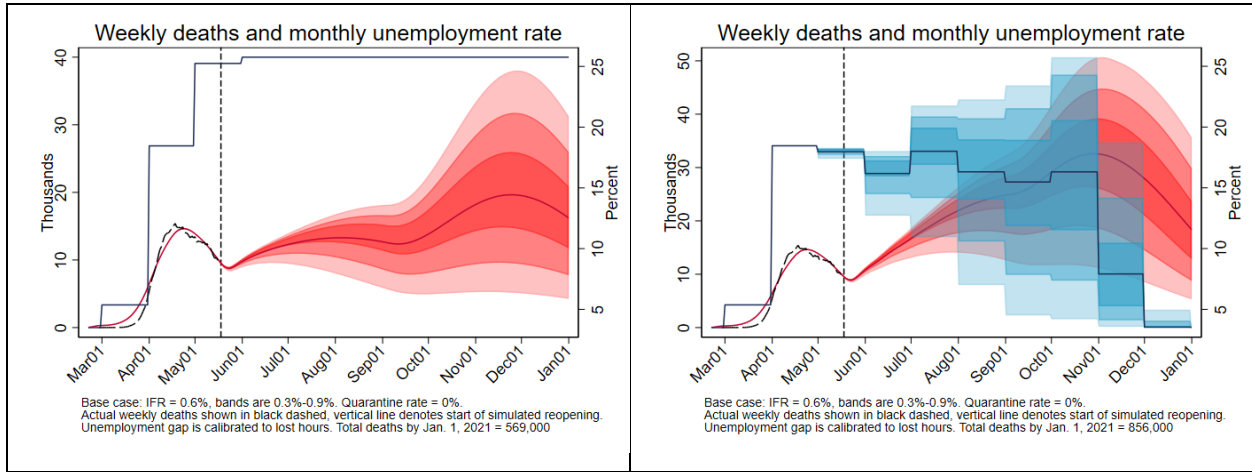


Figure 13. Reopening schools with protections and relaxed non-work social distancing, slow (left) and fast (right) baselines



We also consider a NPI with heightened protections targeted at the elderly. In doing so we follow Acemoglu et al. (2020), who examine a strict protection policy for the old. Specifically, we consider restricting contacts between individuals aged 75+ and others by 75%, relative to the pre-COVID-19 baseline (they consider an extended lockdown for ages 65+). Those eliminated contacts including shopping and non-home visits with friends and family. They also include contacts that are more difficult to restrict, in particular health care workers who provide services to the elderly. A 75% reduction of contacts should thus be interpreted as those individuals comprising necessary other contacts taking strong protective measures including personal protective equipment. We find that this restriction leads to a reduction in deaths among the elderly by just over 5,000 between May 18 and January 1, a 25% reduction in deaths in this age group (we do not provide figures because they are visually close to Figure 4). Because this action reduces contacts between the elderly and other ages substantially, there is a negligible change in deaths in other ages. The reduced deaths allow the governor to reopen more quickly, with the unemployment rate being 0.4pp lower in September with these additional protections for the elderly. There is logic for this within our age-based model: as workers return to work, some get infected, but they have lower mortality risk than the old, and sequestering the old allows those working to return to work sooner. The assumptions underlying our simulation and those in Acemoglu et al. (2020) are quite different, in particular in our baseline total deaths are controlled to a much greater extent than in the much more lethal Acemoglu et al baseline, so they find much

larger mortality reductions than we do. In addition, our simulation starts from a May 18 baseline, in which there already is a pool of infections among the elderly, and end after just over 7 months. Despite these differences, our results are qualitatively consistent with their conclusion that measure aimed specifically at protecting the elderly can save lives; moreover, in our framework, those measures also make room for the economic reopening.

6.3. Testing, tracing, and quarantine

The roadmaps stress the importance of having testing, tracing, and quarantine in place. Currently those capabilities are very limited and remain hampered by availability of testing. Our final simulations examine the possibility that a partial testing, tracing, and quarantine program is put in place in mid-July.

Even a robust program of testing, tracing, and quarantine is likely to be only partially effective. Because of the short latency period, individuals must be identified quickly, then (barring mandatory enforced quarantine) they must comply with self-isolation recommendations. We therefore consider a program in which 20% of the infected are placed into self-isolation at some point during the period of their infection, at which point they self-isolate. Alternatively, this is equivalent to 40% being detected at some point during their infection, but with 50% compliance with self-isolation guidelines.

We repeat the experiments in Figure 12, school reopening, and in Figure 13, school reopening with relaxed social distancing, under the assumption of 20% quarantine; the results are shown in Figure 14 and Figure 15, respectively. If schools remain closed, 20% quarantine effectively allows a brisk reopening of the economy even if social distancing is relaxed, under both the slow and fast governors. If schools reopen with strict protections at school, quarantine brings deaths under control, but at the cost of the governor being unwilling to re-open the economy. Thus, even with quarantine, the governor faces the choice of reopening the economy or reopening school, if citizens relax social distancing. In the fast scenario, the governor still backtracks on the economic reopening in the fall, although the extent of that backtracking depends heavily on the actual (unknown) IFR.

Figure 14. Reopening schools with protections and strict social distancing, slow (left) and fast (right) baselines, 20% quarantine

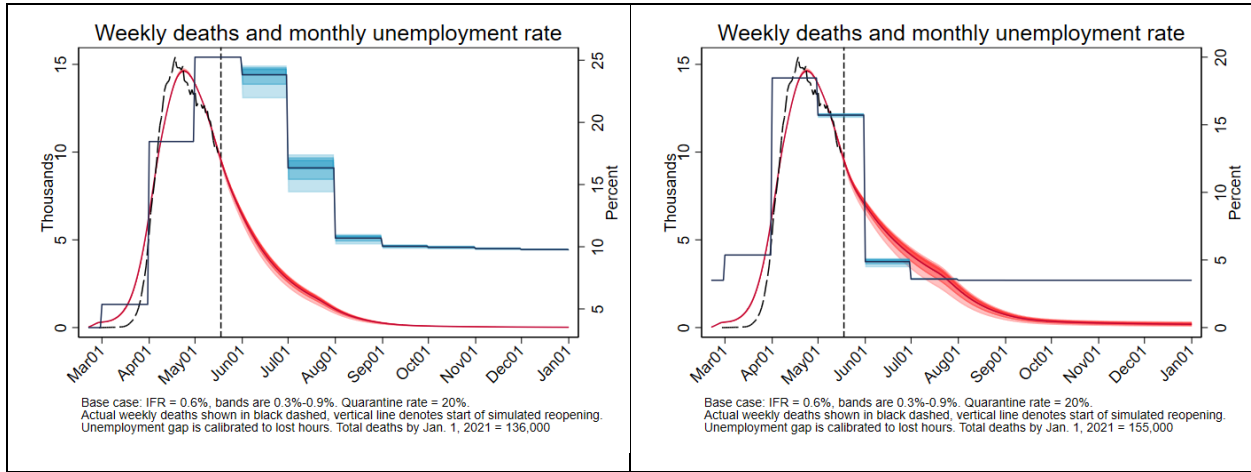
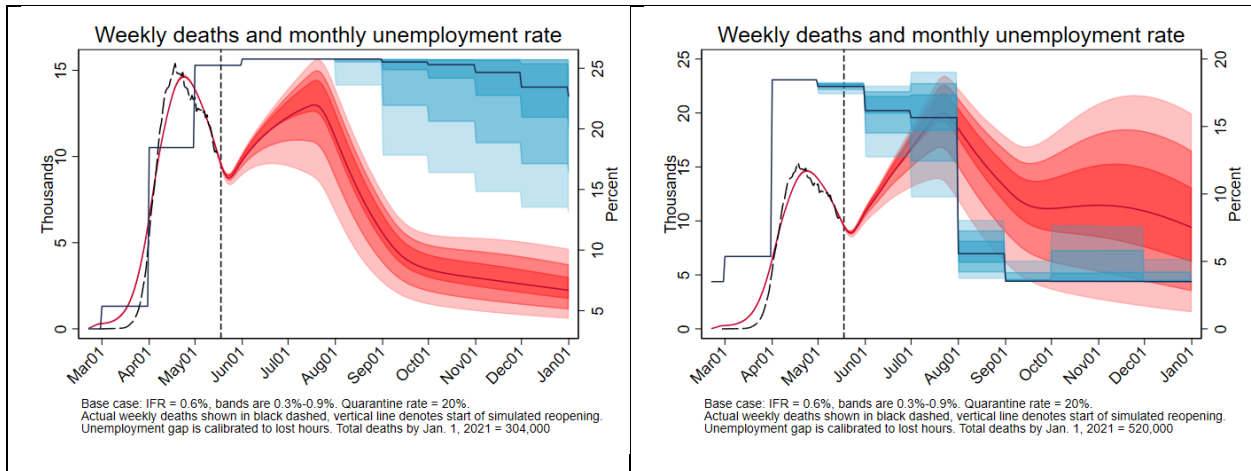


Figure 15. Reopening schools with protections and relaxed non-work social distancing, slow (left) and fast (right) baselines, 20% quarantine



7. Discussion

There are many caveats to and extensions of this work. On the epidemiological side, the situation is far more complex than is captured by our national SEIQRD model. For example, the spread of the epidemic varies regionally, in practice networks matter, and this model does not capture super-spreaders.

On the economic side, the linear input-output structure simplifies more complicated dynamics including nonlinearities and unemployment caused by demand shocks and inflexible prices, and here especially there is more work to be done to incorporate these features (see Baqaee and Farhi (2020a, b)). In particular, if we incorporate more realistic complementarities along supply chains, there will be a force for synchronized reopening, further cutting against a staged reopening.

Additional work also remains examining non-work NPIs, which we find to play a key role in enabling the economic reopening. For example, using the contact survey database, we hope to examine the effect of reductions in specific high-contact non-work activities such as going to bars and large gatherings.

One conclusion we have not stressed, but is evident in many of the simulation figures, is that there is tremendous uncertainty because of the lack of information on the infection-fatality ratio. Obtaining additional information on this, and equivalently on the amount of undetected infections and recovered individuals, would be valuable in guiding policy.

Importantly, by casting the problem as a governor providing guidance or closure restrictions, we abstract from individual behavior about whether to reengage in economic activity and, if so, with what protections from the virus. That said, providing a more expansive interpretation of the governor as representing or following what individual actors are doing simply provides a reinterpretation to the simulations. With this decentralized view, the broad conclusions are the same: if individuals engage in substantial relaxation of social distancing and other non-work protections, then the virus will spread and consumers will again be worried about going shopping and going back to work. In this interpretation too, individual decisions to restrict non-economic exposure leaves room for safely getting back to work.

References

- Acemoglu, D., V. Chernozhukov, I. Werning, and M. Whinston (May 2020). A Multi-Risk SIR Model with Optimally Targeted Lockdown. NBER WP 27102.
- Alvarez, F.E., D. Argente, and F. Lippi (April 2020). A Simple Planning Problem for COVID-19 Lockdown. NBER WP 26981.
- Atkeson, A. (March 2020a). What Will be the Economic Impact of COVID-19 in the US? Rough Estimates of Disease Scenarios. NBER WP 26867.
- Atkeson, A. (April 2020b). How Deadly is COVID-19? Understanding the Difficulties with Estimation of its Fatality Rate. NBER WP 26965.
- Aum, S., S.Y. Lee, and Y. Shin (May 2020). Inequality of Fear and Self-Quarantine: Is There a Trade-Off Between GDP and Public Health? NBER WP 27100.
- Avery, C., W. Bossert, A. Clark, G. Ellison, and S.F. Ellison (April 2020). Policy Implications of Models of the Spread of Coronavirus: Perspectives and Opportunities for Economists. NBER WP 27007.
- Azzimonti, M., A. Fogli, F. Perri and M. Ponder (May 2020). Social Distance Policies in ECON-EPI Networks at https://drive.google.com/file/d/1WmvHk_jxWl7dp4-QB1CifHXPZSkUeRAm/view?usp=sharing
- Baqae, D.R. and E. Farhi (April 2020a). Nonlinear Production Networks with an Application to the COVID-19 Crisis. Manuscript, Harvard University.
- Baqae, D.R. and E. Farhi (May 2020a). Keynesian Production Networks with an Application to the COVID-19 Crisis. Manuscript, Harvard University.
- Baqae, D.R., E. Farhi, M. Mina, and J.H. Stock (May 2020). Evaluating the Economics and Epidemiology of Strategies for Reopening the Economy at <https://drive.google.com/file/d/1O0gMs54RJgQ0nzbygchgP3ewwN45-bB2/view?usp=sharing>
- Berger, D., KI. Herkenhoff, and S. Mongey (2020). An SEIR Infections Disease Model with Testing and Conditional Quarantine. Becker-Friedman Institute WP 2020-25.
- Bloom., N., J. Liang, J. Roberts, and Z.J. Ying (2015). Does Working from Home Work? Evidence from a Chinese Experiment. *The Quarterly Journal of Economics*.

- Boast A., A. Munro, and H. Goldstein (May 15, 2020). An Evidence Summary of Paediatric COVID-19 Literature. *Don't Forget the Bubbles*. Available at: <http://doi.org/10.31440/DFTB.24063>
- Bodenstein, M., G. Corsetti, and L. Guerrieri (April 2020). Social Distancing and Supply Disruptions in a Pandemic. FEDS Discussion Paper 2020-031.
- Çakmakli, C., S. Demiralp, Ş.K. Özcan, and S. Yeşiltaş (May 2020). COVID-19 and Emerging Markets: An Epidemiological Multi-Sectoral Model for a Small Open Economy with an Application to Turkey. Manuscript, Koç University.
- Dingel, J. and B. Neiman (March 2020). How Many Jobs Can be Done at Home? White Paper, Becker-Friedman Institute, University of Chicago.
- Eichenbaum, M.S., S. Rebelo, and M. Trabandt (March 2020). The Macroeconomics of Epidemics. NBER Working Paper 26882.
- Farboodi, M., G. Jarosch, and R. Shimer (April 2020). Internal and External Effects of Social Distancing in a Pandemic. NBER WP 27059.
- Favero, C., A. Ichino, and A. Rustichini (April 2020). Restarting the Economy while Saving Lives under COVID-19. CEPR Discussion Paper DP14664.
- Glover, A., J. Heathcote, D. Krueger, and J-V. Ríos-Rull (April 2020). Health versus Wealth: On the Distributional Effects of Controlling a Pandemic. NBER WP 27046.
- Gottlieb, S., C. Rivers, M.B. McClellan, L. Silvis, and C. Watson (March 2020), National Coronavirus Response: A Road Map to Reopening. American Enterprise Institute at <https://www.aei.org/research-products/report/national-coronavirus-response-a-road-map-to-reopening/>.
- Guerrieri, V., G. Lorenzoni, L. Straub, and I. Werning (April 2020), Macroeconomic Implications of COVID-19: Can Negative Supply Shocks Cause Demand Shortages? NBER WP 26918.
- Hay, J.A., D.J. Haw, W.P. Hanage, C.J.E. Metcalf, and M.J. Mina (2020). Implications of the Age Profile of the Novel Coronavirus, manuscript, March 2020.
- Howard, J. et al. (2020). Face Masks Against COVID-19: An Evidence Review. Preprint at <https://www.preprints.org/manuscript/202004.0203/v2>.
- Jones, C.J., T. Philippon, and V. Venkateswaran (April 2020). Optimal Mitigation Policies in a Pandemic: Social Distancing and Working from Home.” NBER WP 26984.

- Kaiser Family Foundation (2020), State Data and Policy Actions to Address Coronavirus, last updated April 22, 2020 at <https://www.kff.org/health-costs/issue-brief/state-data-and-policy-actions-to-address-coronavirus/>
- Krueger, D., H. Uhlig, and T. Xie (April 2020). Macroeconomic Dynamics and Reallocation in an Epidemic. NBER WP 27047.
- Li, R. et. al. (2020)., Substantial Undocumented Infection Facilitates the Rapid Dissemination of Novel Coronavirus (SARS-CoV2), *Science*, published online March 16, 2020 DOI: 10.1126/science.abb3221 at <https://science.sciencemag.org/content/early/2020/03/13/science.abb3221>.
- Qui, J. (2020). Covert Coronavirus Infections Could Be Seeding New Outbreaks, *Nature News*, posted online March 20,2020 at <https://www.nature.com/articles/d41586-020-00822-x>.
- Lin, Z. and C.M. Meissner (May 2020). Health vs Wealth? Public Health Policies and the Economy during COVIDC-19. NBER WP 27099.
- Ludvigson, S.C., S. Ma, and S. Ng (April 2020). COVID19 and the Macroeconomic Effects of Costly Disasters. NBER WP 26987.
- Magnus, J. (1985). On Differentiating Eigenvalues and Eigenvectors. *Econometric Theory* 1, 179-191.
- Mas, A. and A. Pallais (2019). Alternative Work Arrangements. Forthcoming, *Annual Review of Economics*.
- Moser, C.A. and P. Yared (April 2020). Pandemic Lockdown: The Role of Government Commitment. NBER WP 27062.
- Mongey, S., L. Pilossoph, and A. Weinberg (April 2020), Which Workers Bear the Burden of Social Distancing Policy? Manuscript, University of Chicago.
- Mossong J, Hens N, Jit M, Beutels P, Auranen K, Mikolajczyk R, Massari M, Salmaso S, Tomba GS, Wallinga J, Heijne J, Sadkowska-Todys M, Rosinska M, Edmunds WJ (2017). POLYMOD Social Contact Data. doi: 10.5281/zenodo.1157934 (URL: <https://doi.org/10.5281/zenodo.1157934>), Version 1.1.
- Mulligan, C.B. (April 2020). Economic Activity and the Value of Medical Innovation During a Pandemic. NBER WP 27060.
- Mizumoto, K. et. al., Estimating the Asymptomatic Proportion of Coronavirus Disease 2019 (COVID-19) Cases on Board the Diamond Princess Cruise Ship, Yokohama, Japan,

- 2020,” *Eurosurveillance* 25(10), March 12, 2020 at <https://www.eurosurveillance.org/content/10.2807/1560-7917.ES.2020.25.10.2000180>.
- National Governors’ Association (April 21, 2020). Roadmap to Recovery: A Public Health Guide for Governors. At <https://www.nga.org/center/publications/health/roadmap-to-recovery/>.
- Nishiura, H. et. al. (2020), Estimation of the Asymptomatic Ratio of Novel Coronavirus Infections (COVID-19), forthcoming, *International Journal of Infectious Disease*, posted online February 13, 2020 at <https://doi.org/10.1016/j.ijid.2020.03.020>.
- Rampini, A. (April 2020). Sequential Lifting of COVID-19 Interventions with Population Heterogeneity. NBER WP 27063.
- Rio-Chanona, R.M., P. Mealy, A. Pichler, F. Lafond, and J.D. Farmer (April 14, 2020). Supply and Demand Shocks in the COVID-19 Pandemic: An Industry and Occupation Perspective, Institute for New Economic Thinking Oxford Working Paper 2020-05.
- Romer, P. (April 23, 2020). Roadmap to Responsibly Reopen America.
- Stock, J.H. (March 2020). Data Gaps and the Policy Response to the Novel Coronavirus. NBER WP 26902.
- The Conference Board (April 28, 2020). A Realistic Blueprint for Reopening the Economy by Sector while Ramping Up Testing,” at <https://www.ced.org/2020-solutions-briefs/a-realistic-blueprint-for-reopening-the-economy-by-sector-while-ramping-up>.
- Towers, S. and Z. Feng (2012). Social Contact Patterns and Control Strategies for Influenza in the Elderly. *Mathematical Biosciences* 240, 241-249.
- Vogel, G. and J. Couzin-Frankel (May 4, 2020). Should Schools Reopen? Kids’ Role in Pandemic Still a Mystery. *Science* doi:10.1126/science.abc6227 at <https://www.sciencemag.org/news/2020/05/should-schools-reopen-kids-role-pandemic-still-mystery>.
- Wang, C. et. al. (2020), Evolving Epidemiology and Impact of Non-pharmaceutical Interventions on the Outbreak of Coronavirus Disease 2019 in Wuhan, China, March 6, 2020 at <https://www.medrxiv.org/content/10.1101/2020.03.03.20030593v1>.
- White House and the Centers for Disease Control (April 27, 2020). Testing Blueprint: Opening Up America Again. at <https://www.whitehouse.gov/wp-content/uploads/2020/04/Testing-Blueprint.pdf>.

Appendix Table 1
Standardized Index of Relative Industry Contributions θ

NAICS	Sector	θ
523	Securities, commodity contracts, and investments	2.85*
5411	Legal svcs	2.85*
55	Mgmt of companies and enterprises	2.85*
5415	Computer systems design and related svcs	2.85
211	Oil and gas extraction	2.69
511	Publishing inds, exc internet (includes software)	2.58
524	Insurance carriers and related atvs	1.47
5412OP	Misc professional, scientific, and technical svcs	1.18
334	Computer and electronic products	0.74
331	Primary metals	0.60
315AL	Apparel and leather and allied products	0.48
ORE	Other real estate	0.43
332	Fabricated metal products	0.25
514	Data processing, internet publishing, and other info svcs	0.23
42	Wholesale trade	0.20
325	Chemical products	0.18
326	Plastics and rubber products	0.14
322	Paper products	0.13
313TT	Textile mills and textile product mills	0.07
335	Electrical equipment, appliances, and components	0.03
113FF	Forestry, fishing, and related atvs	-0.01
482	Rail transportation	-0.11
324	Petroleum and coal products	-0.15
333	Machinery	-0.16
22	Utilities	-0.16
486	Pipeline transportation	-0.18
323	Printing and related support atvs	-0.23
532RL	Rental and leasing svcs, lessors of intangibles	-0.27
441	Motor vehicle and parts dealers	-0.30
327	Nonmetallic mineral products	-0.31
3364OT	Other transportation equipment	-0.31
493	Warehousing and storage	-0.32
213	Support atvs for mining	-0.35
521CI	Federal Reserve banks, credit intermed, and related atvs	-0.36
111CA	Farms	-0.36
513	Broadcasting and telecommunications	-0.37
311FT	Food and beverage and tobacco products	-0.39
212	Mining, exc oil and gas	-0.41
483	Water transportation	-0.41

321	Wood products	-0.45
487OS	Other transportation and support atvs	-0.45
337	Furniture and related products	-0.55
4A0	Other retail	-0.56
3361MV	Motor vehicles, bodies and trailers, and parts	-0.57
339	Misc manufacturing	-0.57
HS	Housing	-0.57
562	Waste mgmt and remediation svcs	-0.59
512	Motion picture and sound recording inds	-0.59
561	Administrative and support svcs	-0.61
481	Air transportation	-0.61
452	General merchandise stores	-0.63
81	Other svcs, exc govmt	-0.64
23	Construction	-0.67
445	Food and beverage stores	-0.67
721	Accommodation	-0.68
711AS	Performing arts, sports, museums, and related atvs	-0.68
621	Ambulatory health care svcs	-0.69
622	Hospitals	-0.71
484	Truck transportation	-0.74
623	Nursing and residential care facilities	-0.75
713	Amusements, gambling, and recreation inds	-0.76
722	Food svcs and drinking places	-0.77
525	Funds, trusts, and other financial vehicles	-0.78
624	Social assistance	-0.78
485	Transit and ground passenger transportation	-0.80
61	Educational svcs	-0.81

a*Truncated to take on fourth-highest value